NIH Public Access
Author Manuscript
Nat Cell Biol. Author manuscript; available in PMC 2010 June 29.

Published in final edited form as:
Nat Cell Biol. 2005 October ; 7(10): 1021–1028. doi:10.1038/ncb1302.

The endoplasmic reticulum gateway to apoptosis by Bcl-X_L modulation of the $InsP_3R$

Carl White[1,5], **Chi Li**[2,5], **Jun Yang**[1], **Nataliya B. Petrenko**[1], **Muniswamy Madesh**[2,3], **Craig B. Thompson**[2], and **J. Kevin Foskett**[1,4,6]

[1]Department of Physiology, University of Pennsylvania, Philadelphia, PA 19104, USA.

[2]Department of Cancer Biology, Abramson Family Cancer Research Institute, University of Pennsylvania, Philadelphia, PA 19104, USA.

[3]Institute for Environmental Medicine, University of Pennsylvania, Philadelphia, PA 19104, USA.

[4]Department of Cell and Developmental Biology, University of Pennsylvania, Philadelphia, PA 19104, USA.

Abstract

Members of the Bcl-2 protein family modulate outer mitochondrial membrane permeability to control apoptosis[1,2]. However, these proteins also localize to the endoplasmic reticulum (ER), the functional significance of which is controversial[3, 4]. Here we provide evidence that anti-apoptotic Bcl-2 proteins regulate the inositol 1,4,5-trisphosphate receptor ($InsP_3R$) ER Ca^{2+} release channel resulting in increased cellular apoptotic resistance and enhanced mitochondrial bioenergetics. Anti-apoptotic Bcl-X_L interacts with the carboxyl terminus of the $InsP_3R$ and sensitizes single $InsP_3R$ channels in ER membranes to low [$InsP_3$], enhancing Ca^{2+} and $InsP_3$-dependent regulation of channel activity *in vitro* and *in vivo*, reducing ER Ca^{2+} content and stimulating mitochondrial energetics. The pro-apoptotic proteins Bax and tBid antagonize this effect by blocking the biochemical interaction of Bcl-X_L with the $InsP_3R$. These data support a novel model in which Bcl-X_L is a direct effector of the $InsP_3R$, increasing its sensitivity to $InsP_3$ and enabling ER Ca^{2+} release to be more sensitively coupled to extracellular signals. As a consequence, cells are protected against apoptosis by a more sensitive and dynamic coupling of ER to mitochondria through Ca^{2+}-dependent signal transduction that enhances cellular bioenergetics and preserves survival.

A central feature of molecular models of apoptosis is the control of outer mitochondrial membrane permeability by Bcl-2-related proteins. The pro-apoptotic Bcl-2-related proteins Bax and Bak are required to initiate cytochrome *c* release from mitochondria in response to diverse apoptotic stimuli[1,5]. Anti-apoptotic properties of Bcl-2 and Bcl-X_L have been attributed to their ability to antagonize Bax/Bak by forming heterodimers that prevent their oligomerization and apoptosis initiation[6]. Pro- and anti-apoptotic Bcl-2 proteins also localize to the ER[3,7], and it is now recognized that the ER has an important role in regulating apoptosis[8,9]. The ER is thought to contribute to apoptosis through its role as the principle Ca^{2+} storage organelle in cells[8–11]. At physiological levels, Ca^{2+} released from the ER during

© 2005 Nature Publishing Group

[6]Correspondence should be addressed to J.K.F. (foskett@mail.med.upenn.edu).
[5]These authors contributed equally to this work.

Note: Supplementary Information is available on the Nature Cell Biology website.

COMPETING FINANCIAL INTERESTS
The authors declare that they have no competing financial interests.

NIH-PA Author Manuscript
NIH-PA Author Manuscript
NIH-PA Author Manuscript

NIH-PA Author Manuscript

NIH-PA Author Manuscript

NIH-PA Author Manuscript

cell activation is taken up by mitochondria to stimulate oxidative phosphorylation and enhance ATP production[12]. However, sustained and complete release of ER Ca^{2+} can initiate Ca^{2+}-dependent forms of apoptosis by activating calpain processing of caspase 12 (ref. 13) or by triggering the opening of the mitochondrial permeability transition pore14. It has been suggested that high levels of ER Ca^{2+} may sensitize cells to these pathways of apoptosis by providing a higher quantity of released Ca^{2+} (ref. 11).

Recent evidence suggests that Bcl-2-related proteins can localize to the ER and the nuclear envelope[3] to regulate permeabilities of these membranes as well as those of mitochondria[7]. However, the effects of this localization have not led to a consistent set of observations that link the functions of these proteins, ER Ca^{2+} dynamics and apoptosis control[4]. Genetic studies have suggested that pro-apoptotic Bax and Bak can promote Ca^{2+} release from the ER and initiate a caspase 12-associated form of apoptosis[7], whereas anti-apoptotic Bcl-2 overexpression also promotes Ca^{2+} release by causing an unregulated ER Ca^{2+} leak[15]. Physiological studies are also conflicting regarding the effects of Bcl-2 proteins on Ca^{2+} leakage[4,11] and $InsP_3R$ activity[16]. The nature of Bcl-2-associated ER regulation and the effect that this regulation has on apoptosis are therefore uncertain, prompting us to utilize distinct approaches to investigate the ability of the anti-apoptotic Bcl-2 family member Bcl-X_L to interact with the $InsP_3R$ and regulate Ca^{2+} release, ER $[Ca^{2+}]$ ($[Ca^{2+}]_{ER}$) and apoptosis.

In *in vitro* pull-down assays, full-length human Bcl-X_L interacted with all three mammalian $InsP_3R$ isoforms (Fig. 1a). Immunoprecipitation of Bcl-X_L coprecipitated type 3 $InsP_3R$ from COS-7 cell lysates (Fig. 1a), suggesting that the endogenous proteins interact *in vivo*. Bcl-2 also binds to $InsP_3R$ (see Supplementary Information, Fig. S1), consistent with previous findings[16]. The interacting region in the $InsP_3R$ was localized to the C-terminal region of the channel (Fig. 1c).

The functional consequences of the interaction of Bcl-X_L with the $InsP_3R$ were explored by recording single $InsP_3R$ channels in native ER membranes, by patch-clamp electrophysiology of outer membranes of isolated nuclei[17] (Fig. 2a). Robust $InsP_3R$ channel activity (open probability, P_o ~0.7) was observed with pipette solutions facing the cytoplasmic aspect of the channel containing 10 μM $InsP_3$ and 1 μM Ca^{2+}, conditions optimal for channel activation (Ionescu, L., Mak, D.-O.D., C.W. & K.F., unpublished observations) (Fig. 2b). Channels were observed in 80% of patches, with the mean number of active channels per patch (N_A) ~1.8 (Fig. 2c). When $[InsP_3]$ was reduced to 10 nM, channel activity was substantially decreased (P_o ~0.02) (Fig. 2b), consistent with the $[InsP_3]$ dependence of channel gating[17], and N_A was only ~0.1 (Fig. 2c). Addition to the pipette solution of purified recombinant human Bcl-X_L (rBcl-X_L; 1 μM), with biological activity confirmed in cytochrome *c* release assays (see Supplementary Information, Fig. S1), did not affect the P_o or N_A of channels activated by 10 μM $InsP_3$ (data not shown). In contrast, rBcl-X_L markedly increased the number of channels (N_A ~1.0) and gating (P_o ~0.6) activated by 10 nM $InsP_3$, to levels comparable to those observed with saturating $[InsP_3]$ (Fig. 2b, c). The product of P_o and N_A, a measure of total $InsP_3R$-mediated ion flux across the ER membrane, was increased by over two orders of magnitude in the presence of Bcl-X_L (Fig. 2c).

$InsP_3R$ channel activity in nuclei isolated from cells transiently transfected with Bcl-X_L showed enhanced N_A and P_o in 10 nM $InsP_3$ in the absence of added recombinant protein (Fig. 2b, c), demonstrating an *in vivo* physical and functional membrane-delimited interaction between the $InsP_3R$ and Bcl-X_L that was sufficiently strong to survive the nuclear isolation protocol. Bcl-X_L-enhanced channel activities required $InsP_3$ binding because they were not observed in the absence of added $InsP_3$ (Fig. 2b), and the competitive $InsP_3$ inhibitor heparin ablated the effects (data not shown). Gating of $InsP_3$-liganded $InsP_3R$ channels is biphasically regulated by cytoplasmic $[Ca^{2+}]$ ($[Ca^{2+}]_i$) (ref. [17] and Ionescu *et al.* unpublished observations).

NIH-PA Author Manuscript

NIH-PA Author Manuscript

NIH-PA Author Manuscript

Enhanced channel recruitment and gating conferred by either recombinant or expressed Bcl-X_L was manifested between 100 nM and 1.8 μM Ca^{2+} (Fig. 2d). Thus, Bcl-X_L-activated $InsP_3R$ channels retained biphasic $[Ca^{2+}]_i$ regulation. Taken together, these data indicate that Bcl-X_L binding to the C terminus of the $InsP_3R$ allosterically increases the sensitivity of the channel to very low levels of $InsP_3$ that may exist in resting or minimally stimulated cells[18] at physiological $[Ca^{2+}]$. This suggests that the *in vivo* interaction of $InsP_3R$ with Bcl-X_L does not induce an unregulated Ca^{2+} leak but rather increases the dynamic sensitivity of a highly regulated Ca^{2+} permeability of the ER membrane.

Purified recombinant Bax, a multi-domain family member, and tBid, a BH3-only member, each disrupted binding of $InsP_3R$ to GST–Bcl-X_L (Fig. 3a) and abolished the functional effects of expressed Bcl-X_L (Fig. 3b, c). In contrast, neither protein affected gating in the absence of Bcl-X_L (see Supplementary Information, Fig. S2). It has been reported that Bcl-X_L and Bax can form ion channels in artificial membrane systems[19,20]. However, novel conductances were never observed when either Bcl-X_L, Bax, or tBid was present in the patch pipette solution, or when Bcl-X_L was overexpressed, indicating that under the present experimental conditions these proteins do not form ion channels in native ER membranes.

The cell physiological implications of the Bcl-X_L–$InsP_3R$ interaction were evaluated using chicken DT40 B-cell lines expressing either Bcl-X_L or vector alone (Fig. 4a). Stable expression of Bcl-X_L in wild-type DT40 cells (DT40-WT), which express all three $InsP_3R$ isoforms[21], reduced the Ca^{2+} content of the ER (Ca^{2+}_{ER}) by 25% (Fig. 4b), consistent with some previous observations[4,11]. In contrast, stable (Fig. 4b and see Supplementary Information, Fig. S3c) or transient (see Supplementary Information, Fig. S3a, b) Bcl-X_L expression did not affect the Ca^{2+}_{ER} in a DT40 cell line that was genetically deficient in all $InsP_3R$ isoforms (DT40-$InsP_3R$-KO)[21]. Thus, Bcl-X_L-associated reduction of Ca^{2+}_{ER} depends critically on expression of the $InsP_3R$, consistent with the hypothesis that Bcl-X_L-mediated enhanced $InsP_3R$ ligand sensitivity is the molecular basis of the Bcl-2-enhanced ER Ca^{2+} permeability observed previously[22–24].

Next we examined whether lowered Ca^{2+}_{ER} as a consequence of Bcl-X_L expression represents a fundamental control point in the regulation of apoptosis, because it reduces the amount of Ca^{2+} released through the $InsP_3R$ by pro-apoptotic signals. DT40 pre-B cells undergo apoptosis following immunoglobulin receptor crosslinking in a process that recapitulates negative selection[25]. Bcl-X_L blocks B-cell receptor (BCR)-mediated apoptosis[26]. Therefore, we examined antigen-receptor-mediated apoptosis in DT40-WT and DT40-$InsP_3R$-KO cells stably expressing either Bcl-X_L or empty vector. An anti-BCR antibody (anti-IgM) elicited comparable $[Ca^{2+}]_i$ transients in Bcl-X_L-expressing and control wild-type cells (Fig. 4c), whereas no $[Ca^{2+}]_i$ transients were observed in the $InsP_3R$-KO cells[21] (data not shown). DT40-$InsP_3R$-KO cells were resistant to apoptosis compared with DT40-WT cells during the initial 24 h (Fig. 4d), consistent with previous observations[21]. However, the resistance was transient, with apoptosis at later times being independent of $InsP_3R$ expression. Bcl-X_L inhibited apoptosis in both wild-type and $InsP_3R$-KO cells, as expected, because Bcl-X_L has ER-independent (mitochondrial) mechanisms of action. We reasoned that if Bcl-X_L was anti-apoptotic because it lowered Ca^{2+}_{ER} and therefore reduced the amount of Ca^{2+} that could be conveyed from the ER to mitochondria following $InsP_3R$ activation[9,11], then $InsP_3R$-KO cells expressing Bcl-X_L should have maximal protection against apoptosis because they lack the mechanism ($InsP_3R$) to convey Ca^{2+} from the ER to mitochondria. Surprisingly, the anti-apoptotic action of Bcl-X_L was significantly greater in DT40-WT cells compared with $InsP_3R$-KO cells (Fig. 4d and see Supplementary Information, Fig. S3c). These data demonstrate that the presence of $InsP_3R$ is required for Bcl-X_L to be fully efficacious as an anti-apoptotic mediator.

NIH-PA Author Manuscript

NIH-PA Author Manuscript

NIH-PA Author Manuscript

The ER is an important control point for apoptotic responses to diverse stimuli[8,9]. Our results provide a molecular mechanism that links the ER, Ca^{2+} and Bcl-2 family proteins to apoptosis, involving the ubiquitous $InsP_3R$ ER Ca^{2+} release channel as a target of a direct effector function of anti-apoptotic Bcl-X_L. This function of Bcl-X_L is antagonized by proapoptotic family members, which conforms to a proposed rheostat model in which the balance of pro- to anti-apoptotic Bcl-2 members regulates apoptosis[10], but differs from the prevailing concept that anti-apoptotic Bcl-2 proteins prevent apoptosis solely by antagonizing pro-apoptotic Bcl-2 family members[2,6]. Whereas this paradigm may account for the competing effects of pro- and anti-apoptotic members at mitochondria, the present results suggest that the converse is true at the ER. Here, the pro-apoptotic family member Bax can reverse the function of Bcl-X_L without affecting ER permeability on its own.

Previous studies that observed reduced $Ca^{2+}{}_{ER}$ in response to Bcl-2 expression or Bax/Bak deficiency concluded that the underlying mechanism is associated with an enhanced ER Ca^{2+} leak[15,22–24]. The current results establish the molecular identity of the enhanced leak to be the $InsP_3R$. It was proposed that phosphorylation status of the type 1 $InsP_3R$ linked Bcl-2 expression to $Ca^{2+}{}_{ER}$ (ref. 15). However, phosphorylation cannot account for the rapid effects of Bcl-X_L on $InsP_3R$ gating observed here, as the experiments were performed with solutions that lacked Mg^{2+} — necessary for phosphorylation reactions — and treatment of nuclei with alkaline phosphatase did not affect the ability of Bcl-X_L to activate channel gating (C.W. & K.F., unpublished observations). The effect of Bcl-X_L expression in lowering $Ca^{2+}{}_{ER}$ has not been consistently observed [4,11]. The current observations demonstrate that this effect of Bcl-X_L is $InsP_3R$-dependent, with Bcl-X_L-stimulated $InsP_3R$ channel activity remaining exquisitely regulated by its ligands $InsP_3$ and Ca^{2+}. Thus, cell-type differences in basal concentrations of these ligands and $InsP_3R$ expression can contribute to the magnitude of the effect of Bcl-2 expression on $Ca^{2+}{}_{ER}$, which might reconcile discrepant published observations.

Previously it was believed that reducing $InsP_3$-mediated ER Ca^{2+} release would protect against Ca^{2+}-induced mitochondrial permeability transition[11,14]. This model may possibly account for the early transient protection observed in the control $InsP_3R$-KO cells (Fig. 4d), but it is insufficient to account for the $InsP_3R$-dependent anti-apoptotic effects of Bcl-X_L observed in DT40 cells. If the sole function of Bcl-X_L at the ER was to lower $[Ca^{2+}]_{ER}$, as a mechanism to protect mitochondria from toxic effects of released Ca^{2+}, then protection afforded by Bcl-X_L should be maximal in the $InsP_3R$-KO cells, where Bcl-X_L can exert its mitochondrial effects[1,2] and the ER is irrelevant because the absence of the release channels prevents delivery of Ca^{2+} to mitochondria. However, $InsP_3R$ expression conferred greater Bcl-X_L-mediated protection. Thus, despite the correlation between reduced $[Ca^{2+}]_{ER}$ and apoptosis resistance observed here and previously[11], the $InsP_3R$ provides an anti-apoptotic signal that cannot be accounted for by reduced mitochondrial Ca^{2+} delivery through its effect on $[Ca^{2+}]_{ER}$.

What is the nature of the anti-apoptotic signal that is conferred by $InsP_3R$ expression? We reasoned that Ca^{2+} released from the ER can enhance mitochondrial function by stimulating the citric-acid cycle and oxidative phosphorylation with consequent production of ATP and other important metabolic intermediates[12]. We speculated that maintenance of cellular metabolic homeostasis by Ca^{2+} activation of mitochondrial metabolism would enable cells to better withstand apoptotic insults. In such a model, Bcl-X_L interaction with the $InsP_3R$ generates $[Ca^{2+}]_i$ signals that enhance cellular bioenergetics that afford apoptosis resistance. In single DT40-WT cells perfused with serum-containing medium, infrequent, spontaneous, transient $[Ca^{2+}]_i$ spikes were observed in fewer than 4% of cells (Fig. 5a, b). In contrast, spontaneous $[Ca^{2+}]_i$ spikes were observed in over 25% of Bcl-X_L-expressing DT40-WT cells and these spikes were consistently of higher frequency (Fig. 5a, b). Similarly, $[Ca^{2+}]_i$ oscillations triggered in response to a low concentration of anti-IgM were observed in more

NIH-PA Author Manuscript

NIH-PA Author Manuscript

NIH-PA Author Manuscript

Bcl-X_L-expressing wild-type cells than in control wild-type cells (see Supplementary Information, Fig. S4), reminiscent of observed Bcl-2 enhancement of ligand-induced $[Ca^{2+}]_i$ oscillations[23]. These spikes represent transient release from ER through $InsP_3R$ because they were absent in DT40-$InsP_3R$-KO cells (Fig. 5a). Thus, Bcl-X_L enhances low-level $InsP_3R$-mediated $[Ca^{2+}]_i$ signalling under resting cellular conditions and during low-level agonist stimulation.

Periodic Ca^{2+} release from the ER can elevate mitochondrial matrix $[Ca^{2+}]$ that stimulates Kreb's cycle dehydrogenases, elevating mitochondrial [NADH][12,27]. Bcl-X_L elevated NAD(P)H levels in both wild-type and $InsP_3R$-KO cells, as observed in other cell types[28], but the enhancement was greater in the cells expressing $InsP_3R$ (Fig. 5c, d). In wild-type cells, the elevated signal was in part due to increased mitochondrial NADH because the FCCP-induced fluorescence decrease from basal levels — although not different from those observed in $InsP_3R$-KO cells — was greater in the Bcl-X_L-expressing cells ($P < 0.05$; $n = 7$), a result that cannot be accounted for by increased numbers of mitochondria (Fig. 4a). Thus, spontaneous Bcl-X_L -dependent $InsP_3R$-mediated $[Ca^{2+}]_i$ signals are correlated with enhanced NAD(P)H levels, consistent with these $[Ca^{2+}]_i$ signals stimulating mitochondrial dehydrogenases[27] under resting conditions. Although anti-IgM induced similar $[Ca^{2+}]_i$ signals in wild-type cells in either the presence or absence of Bcl-X_L (Fig. 4b), NAD(P)H fluorescence was unchanged in the Bcl-X_L-transfected wild-type cells (Fig. 5c,d), whereas it was enhanced in the control wild-type cells (Fig. 5c) to levels closer to those achieved in the Bcl-X_L-transfected cells (Fig. 5c), with kinetics correlated with the BCR-induced $InsP_3R$-mediated $[Ca^{2+}]_i$ signal (Fig. 4b). These results suggest either that mitochondrial dehydrogenases in the Bcl-X_L-transfected wild-type cells were already maximally stimulated under resting conditions, or that Ca^{2+}-stimulated NADH production was well compensated by increased oxidation with higher flux through the electron transport chain in these cells. In $InsP_3R$-KO cells, anti-IgM elicited neither a $[Ca^{2+}]_i$ response (data not shown) nor a stimulation of NAD(P)H fluorescence (Fig. 5c, d), demonstrating that the stimulation observed in wild-type cells was mediated by ER Ca^{2+} release. Similar results were obtained in different cell clones (see Supplementary Information, Fig. S4c). Thus, these results suggest that Bcl-X_L enables mitochondria to cope with increased metabolic demand with high efficiency that preserves mitochondrial redox status, dependent upon the $InsP_3R$.

Together the above results suggest that the effects of Bcl-X_L at the ER are anti-apoptotic not only because they minimize the maximal delivery of Ca^{2+} to mitochondria as previously thought, but also because Bcl-X_L facilitates $InsP_3R$-mediated Ca^{2+} delivery to mitochondria that regulates mitochondrial bioenergetics. Such a model is consistent with a general scheme that links cellular resistance to apoptosis with the regulation of cellular metabolism[29,30]. Furthermore, it is consistent with the observation that Bcl-X_L does not stimulate an unregulated leak — which would be energetically costly — but rather modulates the activity of an exquisitely regulated permeability. Nevertheless, because our results do not establish a causal link between enhanced bioenergetics and apoptosis susceptibility, other models are also possible. For example, it may be that the ER Ca^{2+} load *per se*, regulated by the interaction of Bcl-X_L with the $InsP_3R$, rather than Ca^{2+} release, directly determines apoptotic susceptibility. Bcl-X_L interacts with the $InsP_3R$ at the ER membranes and increases its sensitivity to very low levels of $InsP_3$, resulting in increased channel gating and cytoplasmic $[Ca^{2+}]_i$ signals that enhance mitochondrial bioenergetics and increase apoptosis resistance. Anti-apoptotic Bcl-2 family members promote a more dynamic $InsP_3R$ response to achieve more sensitive coupling of Ca^{2+} release to extracellular signals and to increase cell survival. We suggest that Bcl-X_L interaction with the $InsP_3R$ Ca^{2+} release channel is a critical cellular control point that couples the ER to apoptotic pathways. The interaction between Bcl-X_L and $InsP_3R$ may provide a novel therapeutic target, with implications for processes involving apoptosis including cancer, neurodegeneration and cardiovascular disease.

NIH-PA Author Manuscript

NIH-PA Author Manuscript

NIH-PA Author Manuscript

METHODS

Cell culture and transfection

Spodoptera frugiperda (Sf9) cells were maintained in suspension culture at 27 °C in serum-free Sf-900 II SFM media (GIBCO/BLR, Gaithersburg, MD). A baculovirus expression system was used to transiently express Bcl-X_L. COS-7 (*Cercopithecus aethiops* kidney) cells were grown in DMEM/high glucose medium containing 10% (v/v) fetal bovine serum (FBS) (GIBCO/BLR) in a humidified 95/5% air/CO_2 atmosphere. DT40 cells were maintained in suspension culture at 37 °C (95/5% air/CO_2) in RPMI 1640 media (GIBCO/BLR) supplemented with 10% (v/v) FBS, 1% chicken serum, 2 mM glutamine, 100 U ml^{-1} penicillin and 100 μg ml^{-1} streptomycin. Full-length human *Bcl-X_L* cDNA was cloned into pIRES2-DsRed2 vector (Clontech, Palo Alto, CA). Cells were transfected with either empty vector pIRES2-DsRed2 or pBcl-X_L-IRES2-DsRed2 using a Nucleofector Device (Amaxa, Gaithersburg, MD). For selection of stable clones, transfected cells were cultured for 2 weeks in the presence of 2 mg ml^{-1} G418. Transfected cells were identified on the basis of DsRed fluorescence and were further sub-cloned using fluorescence-activated cell sorting (Becton Dickinson, San Jose, CA) into individual wells of a 96-well plate. Bcl-X_L expression was confirmed by western blot and quantified using infrared imaging Odyssey (LI-COR).

Biochemistry

Human *Bcl-X_L* or *Bcl-2* cDNA in pGEX6P-1 (Amersham Pharmacia, Piscataway, NJ) were expressed as GST-fusion proteins in *Escherichia coli* (BL-21; Stratagene, La Jolla, CA) and immobilized on glutathione–Sepharose 4B (Amersham Pharmacia). $InsP_3R$ (type 1) fragments were cloned into pcDNA3.1 or pcDNA3.1/V5 vectors (Invitrogen, Carlsbad, CA). COS-7 cells were transfected (Lipofectamine 2000), and 48–60 h later washed twice with PBS and harvested into 1 ml PBS containing 2% glycerol, 0.05% Triton and protease inhibitor cocktail (Sigma, St Louis, MO). After brief sonication (10 s) and centrifugation, total protein concentration in the lysate was adjusted to 5 mg ml^{-1} and incubated with GST-fusion protein (1 h, 4 °C). Beads were centrifuged, washed three times and prepared for western blot. Co-immunoprecipitation and western blot analysis were performed according to standard protocols.

Baculoviral generation and protein purification

Baculoviruses were generated by first sub-cloning full-length human Bcl-X_L into pVL1393 vector (BD PharMingen, Bedford, MA) with specific tags. pVL1393-flag-Bcl-X_L and pVL1393-his-Bcl-X_L were transfected into Sf9 cells and viral supernatants collected. Viral supernatants were used to infect Sf9 cells until recombinant Bcl-X_L expression was maximized. Flag-tagged Bcl-X_L was purified by anti-FlagM2-agarose affinity beads (Sigma) and eluted by incubation with buffer 0.1 μg ml^{-1} Flag peptide. *Bcl-X_L* cDNA for His-tagged recombinant Bcl-X_L was cloned into pET-16b (Novagen, Madison, WI) and expressed in BL-21, and the resulting His-tagged Bcl-X_L was purified on a Ni-NTA column (Qiagen, Valencia, CA). The plasmid pGEX-4T-1-tBid-his (gift from D. Newmeyer) was transformed into BL-21 and the cell lysate applied to glutathione-Sepharose, digested with thrombin (Novagen; 4 U ml^{-1}, 25 °C, 5 h) and purified using Ni-NTA chromatography. PTYB1-mBax was obtained by inserting mouse *Bax* cDNA into pTYB1 vector (New England Biolabs, Beverly, MA). *E. coli* ER2566 (New England Biolabs) bearing the plasmid pTYB1-mBax were cultured and the fusion protein of Bax–chitin-binding protein was purified using a chitin-affinity column (New England Biolabs). Full-length Bax protein was eluted by incubating with 50 mM DTT at 16 °C for 40 h. All purified recombinant proteins were dialysed in buffer with 20 mM HEPES pH 7.5 and 20% glycerol, and stored at –80 °C. Protein samples for patch-clamping were first dialysed against buffer containing 10 mM HEPES pH 7.3, 140 mM KCl and 10% glycerol, and concentrated using Microcon (Millipore, Bedford, MA) to concentrations higher than 50 μM.

NIH-PA Author Manuscript

NIH-PA Author Manuscript

NIH-PA Author Manuscript

Electrophysiology

Sf9 cells were washed twice with PBS and suspended in a nuclear isolation solution containing: 150 mM KCl, 250 mM sucrose, 1.5 mM β-mercapoethanol, 10 mM Tris-HCl, 0.05 mM phenylmethylsulphonyl fluoride, protease inhibitor cocktail (Complete, Roche Diagnostics, Indianapolis, IN), pH 7.5. Nuclei were isolated using a Dounce glass homogenizer and plated onto a 1-ml glass-bottomed dish containing standard bath solution: 140 mM KCl, 10 mM HEPES and 0.5 mM BAPTA (free $[Ca^{2+}] = 300$ nM), pH 7.1. The pipette solution contained 140 mM KCl, 0.5 mM ATP, 10 mM HEPES, pH 7.1. The free $[Ca^{2+}]$ in all solutions was adjusted to the desired level by the addition of an appropriate Ca^{2+} chelator, as described previously[17]. Experiments were performed at room temperature. Data were acquired using an Axopatch-1D amplifier (Axon Instruments, Union City, CA) and single-channel analysis performed using QuB software (University of Buffalo).

Calcium measurement and apoptosis assay

DT40 cells were plated onto a glass-bottomed perfusion chamber mounted on the stage of an inverted microscope (Nikon Eclipse TE2000) and incubated with Fura-2 AM (Molecular Probes, Eugene, OR; 2 μM) for 30 min at room temperature in normal culture media. Cells were then continuously perfused with Hanks' balanced salt solution (Sigma), containing 1.8 mM $CaCl_2$ and 0.8 mM $MgCl_2$, pH 7.4. In experiments in which calcium oscillations were measured, cells were perfused with complete culture media without phenol. Fura-2 was alternately excited at 340 and 380 nm, and the emitted fluorescence filtered at 510 nm was collected and recorded using a CCD-based imaging system running Ultraview software (Perkin-Elmer, Norwalk, CT). Thapsigargin (Sigma) was applied in Ca^{2+}-free Hanks' solution containing 0.5 mM $LaCl_3$ to block Ca^{2+} extrusion across the plasma membrane[31]. Dye calibration was achieved by applying experimentally determined constants to the standard equation: $[Ca^{2+}] = K_d\,\beta(R-R_{min})/(R_{max}-R)$. Cell viability was determined after application of anti-BCR antibody (IgM; SouthernBiotech, Birmingham, AL) using DAPI staining (1 μg ml^{-1}) and assays were performed on an LSR flow cytometer (Beckton Dickinson).

NAD(P)H measurements

DT40 cells (10×10^6 cells per ml) were suspended in Hanks' balanced salt solution (Sigma). Autofluorescence of NAD(P)H was monitored at 350/460 nm (excitation/emission) using a multi-wavelength excitation, dual-wavelength emission fluorimeter (Delta RAM, PTI , Birmingham, NJ). Experiments were performed at 37 °C.

Analysis and statistics

Data were summarized as the mean ± s.e.m. and the statistical significance of differences between means was assessed using unpaired *t*-tests or analysis of variance (ANOVA) for repeated measures, using Fisher's protected least-significant difference (PLSD) test. Differences between means were accepted as statistically significant at the 95% level ($P < 0.05$).

BIND identifiers

Four BIND identifiers (www.bind.ca) are associated with this manuscript: 331015, 331016, 331017 and 331018.

Supplementary Material

Refer to Web version on PubMed Central for supplementary material.

NIH-PA Author Manuscript

NIH-PA Author Manuscript

NIH-PA Author Manuscript

Acknowledgments

We are grateful to D. Newmeyer for the tBid expression plasmid, and S. Joseph and A. Tanimura for $InsP_3R$ antibodies. C.W. and C.L. contributed equally to the major intellectual and technical aspects of the studies. J.Y. and N.B.P. contributed molecular biological and electrophysiology support, respectively. M.M. performed the NADH assays. C.B.T. and J.K.F. contributed ideas and assisted in the preparation of the text. This work was supported by NIH grants (C.B.T. and J.K.F.), an NIH Training Grant (C.L.), an American Heart Association Fellowship (C.W.) and the Abramson Family Cancer Research Institute.

LETTERS

1. Wei MC, et al. Proapoptotic BAX and BAK: A requisite gateway to mitochondrial dysfunction and death. Science 2001;292:727–730. [PubMed: 11326099]
2. Vander Heiden MG, Thompson CB. Bcl-2 proteins: regulators of apoptosis or of mitochondrial homeostasis? Nature Cell Biol 1999;1:E209–E216. [PubMed: 10587660]
3. Krajewski S, et al. Investigation of the subcellular distribution of the Bcl-2 oncoprotein - residence in the nuclear envelope, endoplasmic reticulum, and outer mitochondrial membranes. Cancer Res 1993;53:4701–4714. [PubMed: 8402648]
4. Distelhorst CW, Shore GC. Bcl-2 and calcium: controversy beneath the surface. Oncogene 2004;23:2875–2880. [PubMed: 15077150]
5. Jurgensmeier JM, et al. Bax directly induces release of cytochrome c from isolated mitochondria. Proc. Natl Acad. Sci. USA 1998;95:4997–5002. [PubMed: 9560217]
6. Antonsson B, et al. Inhibition of Bax channel-forming activity by Bcl-2. Science 1997;277:370–372. [PubMed: 9219694]
7. Zong WX, et al. Bax and Bak can localize to the endoplasmic reticulum to initiate apoptosis. J. Cell Biol 2003;162:59–69. [PubMed: 12847083]
8. Breckenridge DG, Germain M, Mathai JP, Nguyen M, Shore GC. Regulation of apoptosis by endoplasmic reticulum pathways. Oncogene 2003;22:8608–8618. [PubMed: 14634622]
9. Orrenius S, Zhivotovsky B, Nicotera P. Regulation of cell death: the calcium-apoptosis link. Nature Rev. Mol. Cell Biol 2003;4:552–565. [PubMed: 12838338]
10. Scorrano L, et al. BAX and BAK regulation of endoplasmic reticulum Ca^{2+}: A control point for apoptosis. Science 2003;300:135–139. [PubMed: 12624178]
11. Rizzuto R, et al. Calcium and apoptosis: facts and hypotheses. Oncogene 2003;22:8619–8627. [PubMed: 14634623]
12. Duchen MR. Mitochondria and calcium: from cell signalling to cell death. J. Physiol 2000;529:57–68. [PubMed: 11080251]
13. Nakagawa T, Yuan J. Cross-talk between two cysteine protease families. Activation of caspase-12 by calpain in apoptosis. J. Cell Biol 2000;150:887–894. [PubMed: 10953012]
14. Szalai G, Krishnamurthy R, Hajnoczky G. Apoptosis driven by IP_3-linked mitochondrial calcium signals. EMBO J 1999;18:6349–6361. [PubMed: 10562547]
15. Oakes SA, et al. Proapoptotic BAX and BAK regulate the type 1 inositol trisphosphate receptor and calcium leak from the endoplasmic reticulum. Proc. Natl Acad. Sci. USA 2005;102:105–110. [PubMed: 15613488]
16. Chen R, et al. Bcl-2 functionally interacts with inositol 1,4,5-trisphosphate receptors to regulate calcium release from the ER in response to inositol 1,4,5-trisphosphate. J. Cell Biol 2004;166:193–203. [PubMed: 15263017]
17. Mak DO, McBride S, Foskett JK. Inositol 1,4,5-trisphosphate activation of inositol trisphosphate receptor Ca^{2+} channel by ligand tuning of Ca^{2+} inhibition. Proc. Natl Acad. Sci. USA 1998;95:15821–15825. [PubMed: 9861054]
18. Luzzi V, Sims CE, Soughayer JS, Allbritton NL. The physiologic concentration of inositol 1,4,5-trisphosphate in the oocytes of *Xenopus laevis*. J. Biol. Chem 1998;273:28657–28662. [PubMed: 9786859]
19. Korsmeyer SJ, et al. Pro-apoptotic cascade activates BID, which oligomerizes BAK or BAX into pores that result in the release of cytochrome c. Cell Death Differ 2000;7:1166–1173. [PubMed: 11175253]

NIH-PA Author Manuscript

NIH-PA Author Manuscript

NIH-PA Author Manuscript

20. Minn AJ, et al. Bcl-x_L forms an ion channel in synthetic lipid membranes. Nature 1997;385:353–357. [PubMed: 9002522]
21. Sugawara H, Kurosaki M, Takata M, Kurosaki T. Genetic evidence for involvement of type 1, type 2 and type 3 inositol 1,4,5-trisphosphate receptors in signal transduction through the B-cell antigen receptor. EMBO J 1997;16:3078–3088. [PubMed: 9214625]
22. Foyouzi-Youssefi R, et al. Bcl-2 decreases the free Ca^{2+} concentration within the endoplasmic reticulum. Proc. Natl Acad. Sci. USA 2000;97:5723–5728. [PubMed: 10823933]
23. Palmer AE, Jin C, Reed JC, Tsien RY. Bcl-2-mediated alterations in endoplasmic reticulum Ca^{2+} analyzed with an improved genetically encoded fluorescent sensor. Proc. Natl Acad. Sci. USA 2004;101:17404–17409. [PubMed: 15585581]
24. Pinton P, et al. Reduced loading of intracellular Ca^{2+} stores and downregulation of capacitative Ca^{2+} influx in Bcl-2-overexpressing cells. J. Cell Biol 2000;148:857–862. [PubMed: 10704437]
25. Niiro H, Clark EA. Regulation of B-cell fate by antigen-receptor signals. Nature Rev. Immunol 2002;2:945–956. [PubMed: 12461567]
26. Doi T, Motoyama N, Tokunaga A, Watanabe T. Death signals from the B cell antigen receptor target mitochondria, activating necrotic and apoptotic death cascades in a murine B cell line, WEHI-231. Int. Immunol 1999;11:933–941. [PubMed: 10360967]
27. Hajnoczky G, Robb-Gaspers LD, Seitz MB, Thomas AP. Decoding of cytosolic calcium oscillations in the mitochondria. Cell 1995;82:415–424. [PubMed: 7634331]
28. Kowaltowski AJ, Fiskum G. Redox mechanisms of cytoprotection by Bcl-2. Antioxid. Redox. Signal 2005;7:508–514. [PubMed: 15706098]
29. Hammerman PS, Fox CJ, Thompson CB. Beginnings of a signal-transduction pathway for bioenergetic control of cell survival. Trends Biochem. Sci 2004;29:586–592. [PubMed: 15501677]
30. Plas DR, Thompson CB. Cell metabolism in the regulation of programmed cell death. Trends Endocrinol. Metab 2002;13:75–78. [PubMed: 11854022]
31. Shimizu H, Borin ML, Blaustein MP. Use of La to distinguish activity of the plasmalemmal Ca^{2+} pump from Na^+/Ca^{2+} exchange in arterial myocytes. Cell Calcium 1997;21:31–41. [PubMed: 9056075]
32. Haynes LP, Tepikin AV, Burgoyne RD. Calcium-binding protein 1 is an inhibitor of agonist-evoked, inositol 1,4,5-trisphosphate-mediated calcium signaling. J. Biol. Chem 2004;279:547–555. [PubMed: 14570872]

NIH-PA Author Manuscript
NIH-PA Author Manuscript
NIH-PA Author Manuscript

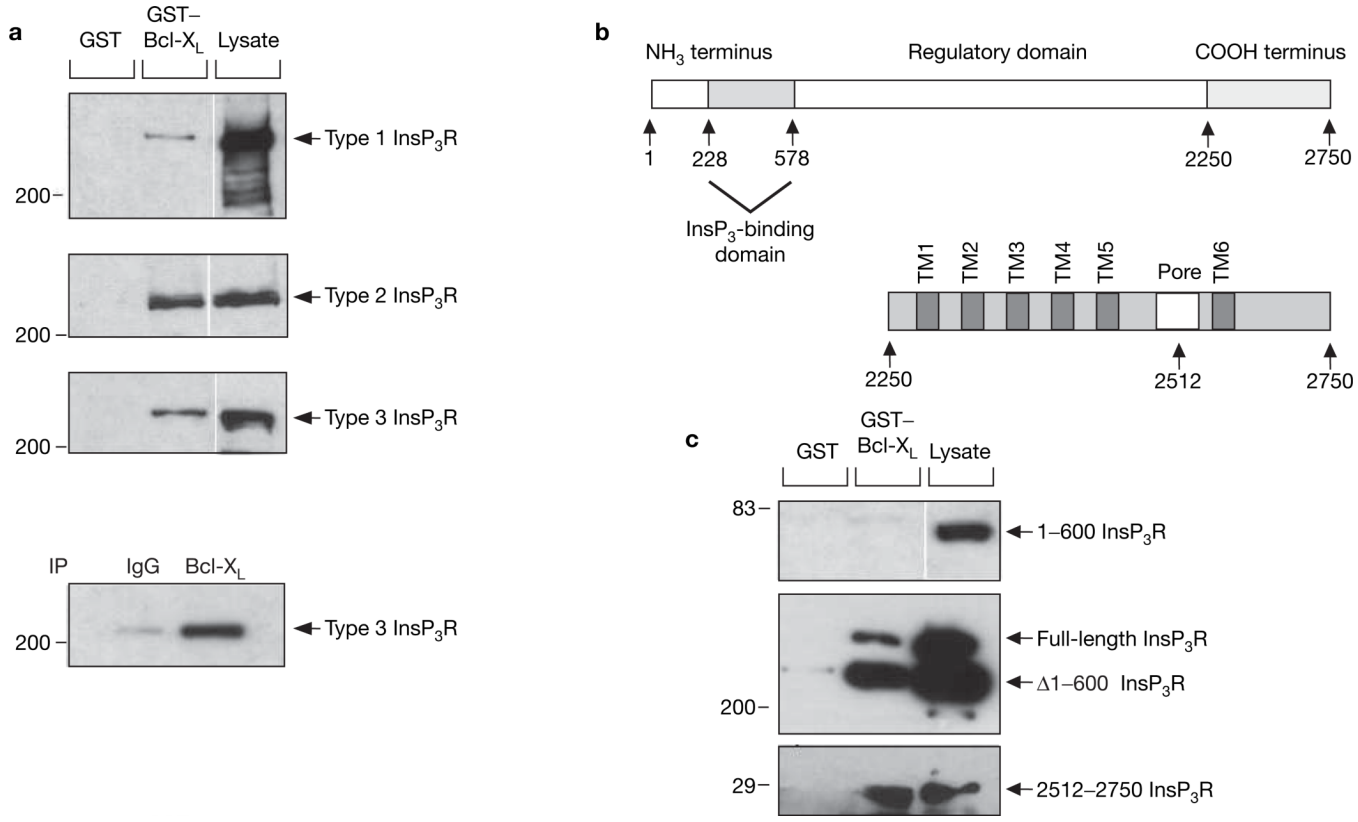

Figure 1.

Interaction of Bcl-X_L with $InsP_3R$. (**a**) Bcl-X_L binds to full-length types 1, 2 and 3 $InsP_3R$. Lysates from DT40-$InsP_3R$-KO cells stably expressing rat type 1 $InsP_3R$ and from COS-7 cells that endogenously express type 2 and type 3 $InsP_3R$, were incubated with GST–Bcl-X_L, and bound $InsP_3R$ was detected with isoform-specific antibodies (top three panels). Bottom panel: co-immunoprecipitation of endogenous Bcl-X_L and type 3 $InsP_3R$ from COS-7 cells. (**b**) Domain structure of full-length $InsP_3R$ and of its C-terminal region. (**c**) Bcl-X_L binds within the C terminus of $InsP_3R$. GST–Bcl-X_L failed to pull-down the V5-tagged 1–600 type 1 $InsP_3R$ fragment expressed in COS-7 cells (top panel). Expression of 1–600 $InsP_3R$ was verified by a western blot of cell lysates with V5-specific antibody (lane 3). Rat type 1 $InsP_3R$ lacking the first 600 residues (Δ1–600 $InsP_3R$) expressed in COS-7 cells was successfully pulled-down along with endogenous $InsP_3R$-1 (middle panel). GST–Bcl-X_L effectively binds to the C-terminal 2512–2750 residues of type 1 $InsP_3R$ (bottom panel). All western blots depicted are representative of three independent experiments.

NIH-PA Author Manuscript

NIH-PA Author Manuscript

NIH-PA Author Manuscript

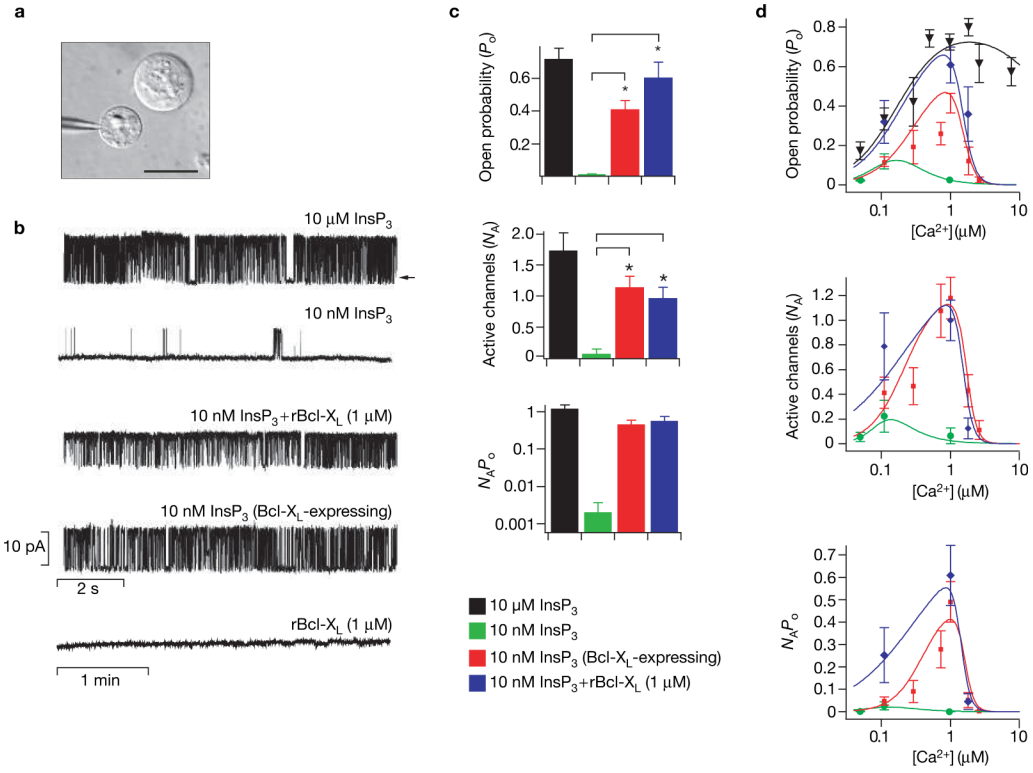

Figure 2.

Effects of Bcl-X_L on $InsP_3R$ single-channel activity. (**a**) Isolated nuclear preparation from Sf9 cells, which endogenously express only type 1 $InsP_3R$. Patch pipette approaching an isolated nucleus with an intact cell visible directly above; scale bar, 15 μM. (**b**) $InsP_3R$ channel activity. Typical $InsP_3R$ single-channel current recordings in the presence of saturating (10 μM) or low (10 nM) $InsP_3$; in the absence or presence of recombinant Bcl-X_L (rBcl-X_L; 1 μM); or with 10 nM $InsP_3$ in cells transiently transfected with Bcl-X_L. Channel activity was not evoked by rBcl-X_L (1 μM) alone. Pipette $[Ca^{2+}]$ was 1 μM, optimal for channel activity[17]; arrow indicates zero current level. (**c**) Summary of the effects of Bcl-X_L on $InsP_3R$ channel activity. In pipettes containing 10 nM $InsP_3$, the open probability (P_o) increased from 0.022 ± 0.001 (n = 2) to 0.61 ± 0.09 (n = 10) with addition of 1 μM rBcl-X_L (n = number of patches used in P_o determination). Similarly, when Bcl-X_L was overexpressed, P_o increased to 0.42 ± 0.05 (n = 11). Bcl-X_L also increased the number of activated channels (N_A). In 10 nM $InsP_3$, N_A was increased from 0.10 ± 0.07 (n = 20) under control conditions to 1.00 ± 0.16 (n = 54) and 1.18 ± 0.17 (n = 61) in the presence of recombinant or expressed Bcl-X_L, respectively. The total ER ion flux as indicated by the product N_AP_o was increased by Bcl-X_L (note log scale). Asterisks indicate $P < 0.001$, unpaired t-test. Both His- and Flag-tagged rBcl-X_L, generated using distinct purification protocols, were equally effective, whereas His-tagged NCS-1, which does not interact with $InsP_3R$ (ref. 32), had no effect either alone or in combination with 10 nM $InsP_3$ (data not shown). (**d**) Dependence of $InsP_3R$ channel activity on $[Ca^{2+}]$ at the cytoplasmic face of the channel. Effect of $[Ca^{2+}]_i$ on P_o, N_A and N_AP_o in the presence of 10 μM $InsP_3$ (black inverted triangles), 10 nM $InsP_3$ (green circles), 10 nM $InsP_3$ + 1 μM rBcl-X_L (blue diamonds) and 10 nM $InsP_3$ + Bcl-X_L expression (red squares).

NIH-PA Author Manuscript

NIH-PA Author Manuscript

NIH-PA Author Manuscript

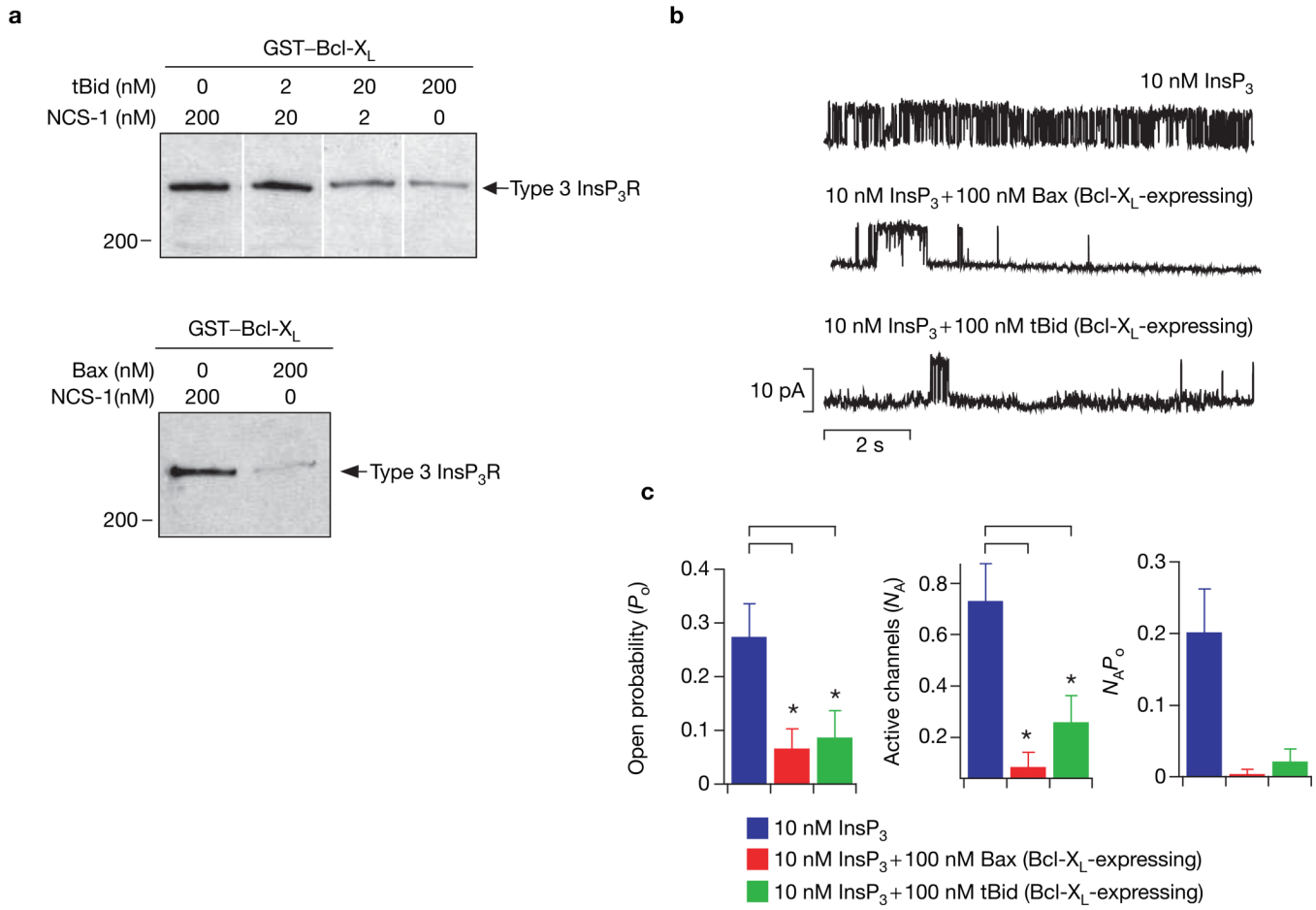

Figure 3.

tBid and Bax antagonize the effects of Bcl-X_L on $InsP_3R$ channel activity. (**a**) tBid and Bax inhibit binding of Bcl-X_L to $InsP_3R$. COS-7 cell lysates were incubated with GST–Bcl-X_L in the absence or presence of recombinant tBid (2–200 nM; upper panel) or recombinant Bax (200 nM; lower panel), and bound $InsP_3R$ was detected with a type 3 antibody. Recombinant neuronal calcium sensor-1 (NCS-1) was used to control for total protein concentration in both experiments. Data are representative of three independent experiments. (**b**) tBid and Bax inhibit the electrophysiological effects of Bcl-X_L. Typical current traces showing the effects of 100 nM recombinant tBid or Bax in the presence of 10 nM $InsP_3$ in nuclei isolated from cells transiently transfected with Bcl-X_L. Pipette [Ca^{2+}] was 1 μM. (**c**) Addition of 100 nM tBid or Bax decreased P_o from 0.28 ± 0.06 (n = 5) to 0.07 ± 0.03 (n = 3) and 0.09 ± 0.05 (n = 3), respectively. Similarly, N_A was reduced from 0.74 ± 0.14 (n = 38) to 0.26 ± 0.10 (n = 33) in the presence of tBid and to 0.09 ± 0.05 (n = 33) in the presence of Bax. The product N_AP_o was also reduced. Asterisks indicate $P < 0.001$, unpaired t-test.

NIH-PA Author Manuscript

NIH-PA Author Manuscript

NIH-PA Author Manuscript

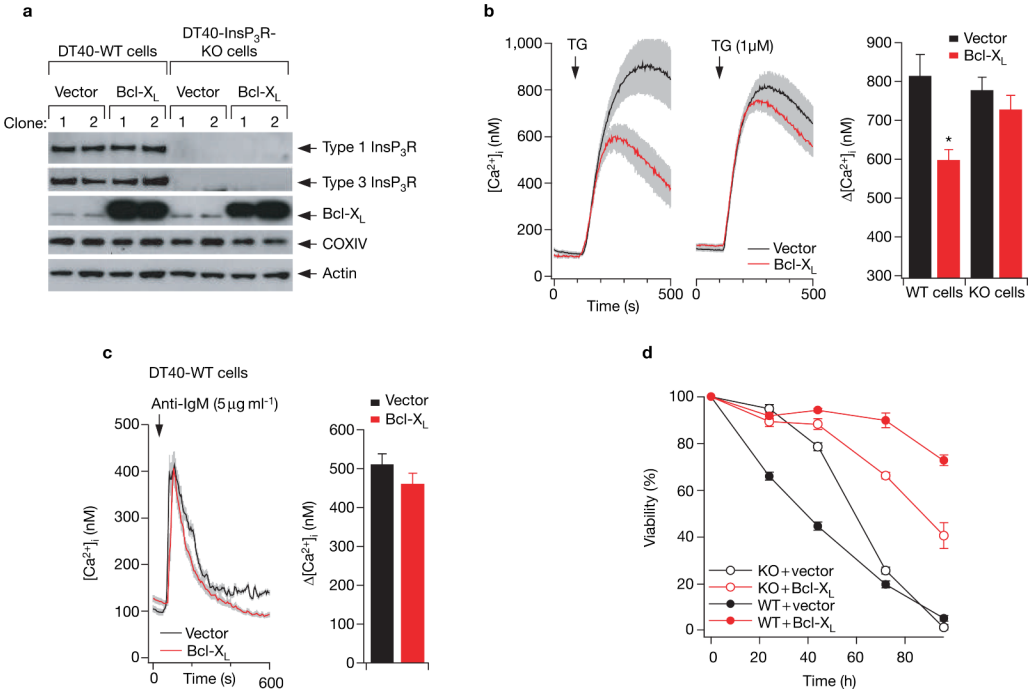

Figure 4.

Interaction of Bcl-X_L with $InsP_3R$ is essential for Bcl-X_L effects on ER Ca^{2+} regulation and inhibition of apoptosis. (**a**) The empty vectors pIRES2-DsRed2 or pBcl-X_L-IRES2-DsRed2 were stably expressed in DT40-WT and DT40-$InsP_3R$-KO cells. Expression levels of types 1 and 3 $InsP_3R$, Bcl-X_L and OxPhos complex IV (COXIV; subunit 1) were examined by western blot. Expression of the mitochondrial complex IV protein was unchanged in the Bcl-X_L-expressing clones. Depicted blots are representative of three independent experiments. (**b**) Effects of Bcl-X_L expression on the Ca^{2+} content of the ER ($Ca^{2+}{}_{ER}$). Typical records depicting change in cytoplasmic $[Ca^{2+}]$ ($[Ca^{2+}]_i$) in response to application of 1 μM thapsigargin (TG) in DT40-WT and DT40-$InsP_3R$-KO cells stably transfected with either Bcl-X_L or vector alone. $Ca^{2+}{}_{ER}$ was indirectly estimated by single-cell imaging of the $[Ca^{2+}]_i$ responses to acute inhibition by thapsigargin of ER Ca^{2+} uptake. Each trace represents mean ± s.e.m. of at least six cells within the image field. Bar graph summarizes the effects of thapsigargin; data represent mean ± s.e.m. for at least 30 cells in multiple trials. Asterisk indicates $P < 0.05$, ANOVA. Mean values of resting $[Ca^{2+}]_i$ ranged from 80 to 100 nM, with no significant differences among duplicate clones of the four cell lines (data not shown). (**c**) $[Ca^{2+}]_i$ transients in response to 5 μg ml^{-1} anti-BCR antibody (anti-IgM) in DT40-WT cells stably transfected with either Bcl-X_L or vector alone. Summary data represent the peak amplitude (mean ± s.e.m.) for at least 30 cells in multiple trials. (**d**) Cell viability after treatment with 20 μg ml^{-1} anti-BCR antibody (anti-IgM) (time 0) of DT40-WT (solid symbols) and DT40-$InsP_3R$-KO (open symbols) cells stably expressing Bcl-X_L (red) or vector alone (same clones as in **b**). Similar results were obtained using independent clones (see Supplementary Information, Fig. S3).

NIH-PA Author Manuscript
NIH-PA Author Manuscript
NIH-PA Author Manuscript

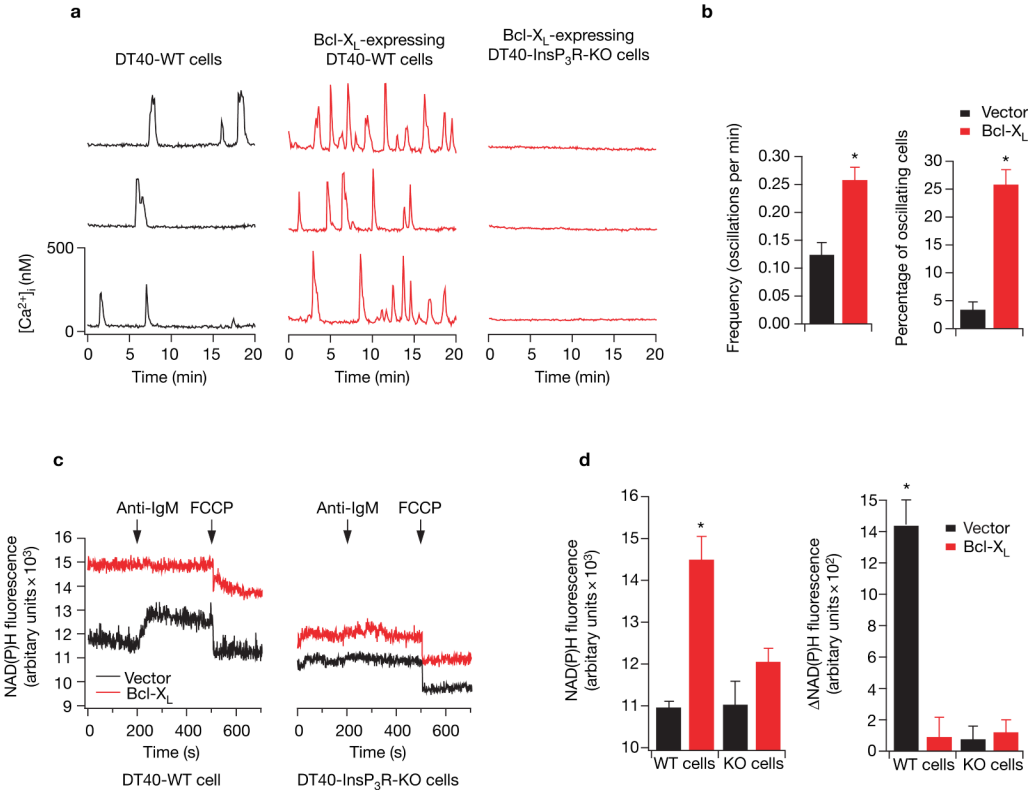

Figure 5.

The Bcl-X_L–$InsP_3R$ interaction modulates $[Ca^{2+}]_i$ signalling and mitochondrial NADH levels. (**a**) Spontaneous $[Ca^{2+}]_i$ oscillations in three representative DT40-WT cells stably expressing vector alone (left) or Bcl-X_L (middle), and DT40-$InsP_3R$-KO cells expressing Bcl-X_L (right). (**b**) The difference in frequency and number of oscillating cells (mean ± s.e.m.) between vector only and Bcl-X_L-expressing cells. (**c**) NAD(P)H fluorescence measurements from DT40-WT and DT40-$InsP_3R$-KO cells expressing Bcl-X_L or vector in response to 5 μg ml^{-1} anti-BCR antibody (anti-IgM) and FCCP (2 μM). The average (± s. e.m.) resting NAD(P)H fluorescence and the change in NAD(P)H fluorescence in response to anti-IgM stimulation for four independent experiments are plotted in **d**. Asterisk indicates $P < 0.001$, ANOVA. Similar results were obtained using independent clones (see Supplementary Information, Fig. S4).